

Supplement contains Figures S1-6 and Tables S1-5.

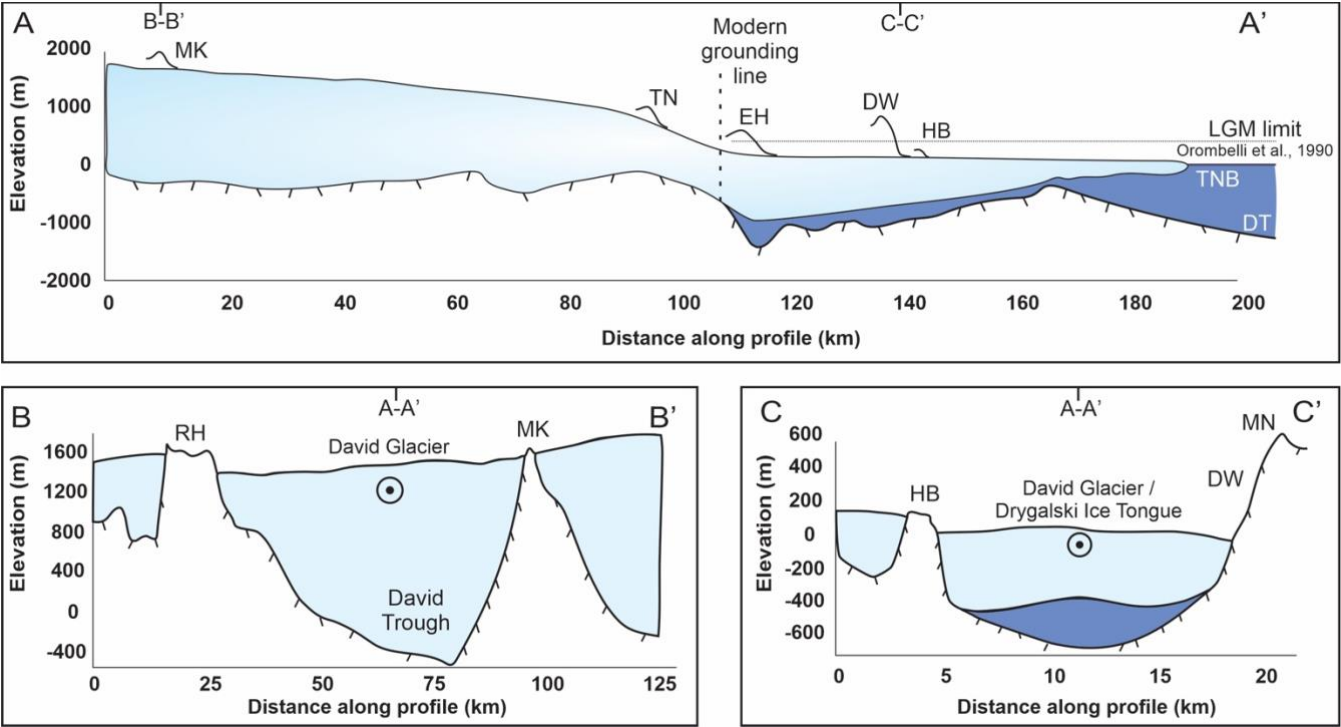


Figure S1: A) Flow parallel cross section showing relationship between field sites and modern surface and bed topography, B) Flow perpendicular cross section through Ricker Hills and Mt. Kring and C) Flow perpendicular cross section through Hughes Bluff and D'Urville Wall. Refer to Fig. 1 for profile locations.

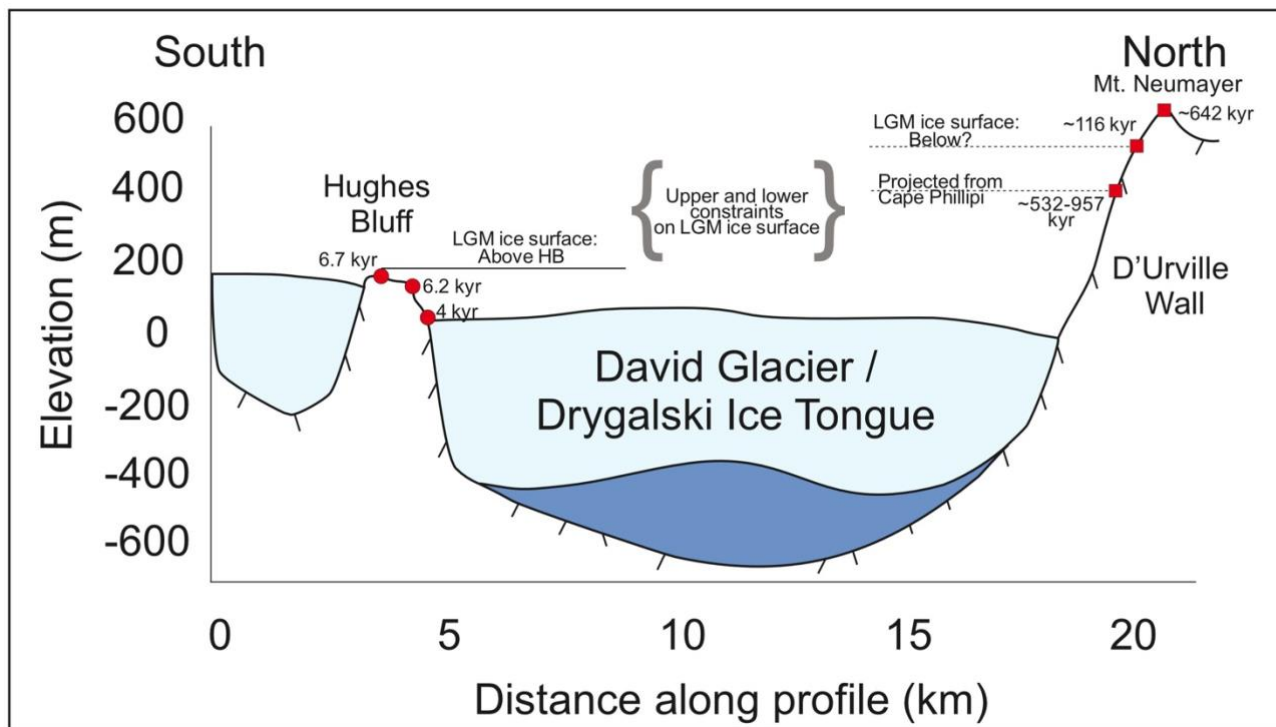


Figure S2: Cross section from Hughes Bluff to Mt. Neumayer combining the high-resolution chronology (red circles) from Hughes Bluff with  $^{10}\text{Be}$  derived exposure ages from high-elevation bedrock samples (red squares). Bedrock ages older than Holocene suggest cold-based ice cover and minimal erosion, and are used as constraints on upper ice surface elevation since the LGM. Elevation data source Howat et al. (2019), bathymetry data source Fretwell et al. (2013).

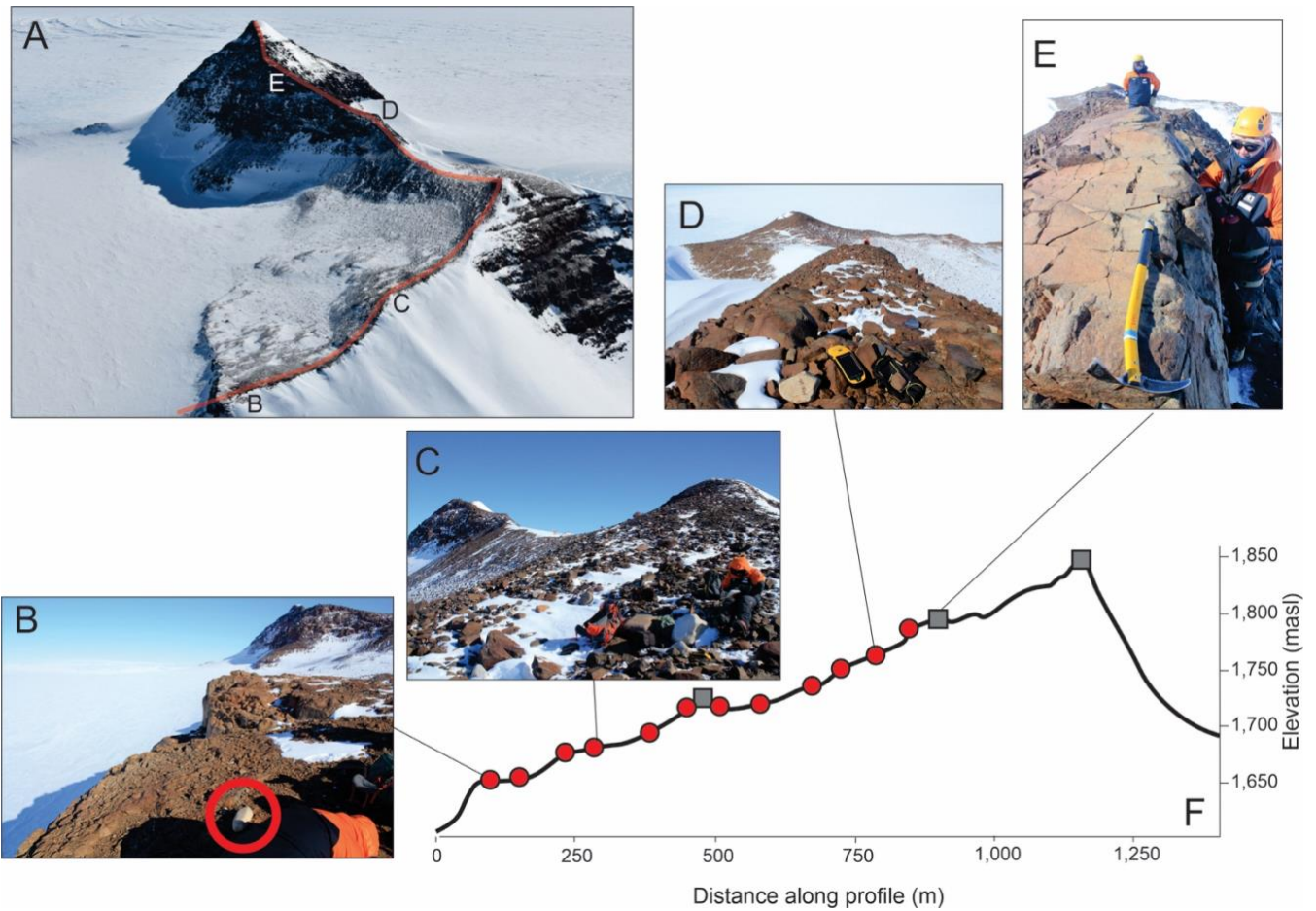


Figure S3: (A) West facing oblique aerial photo of Mt. Kring with approximate location of topographic profile (red), (B) West facing view of lowest elevation site with perched glacial erratics on bedrock, (C) West facing view of scattered glacial till draping bedrock ridge. (D) East facing view of scattered high elevation sandstone erratics perched on fractured bedrock, (E) East facing view from highest elevation striated bedrock outcrop, ice axe parallel to striation direction. (F) Topographic profile from SfMP showing representative sampling sites (red circles for erratics, grey squares for bedrock samples).

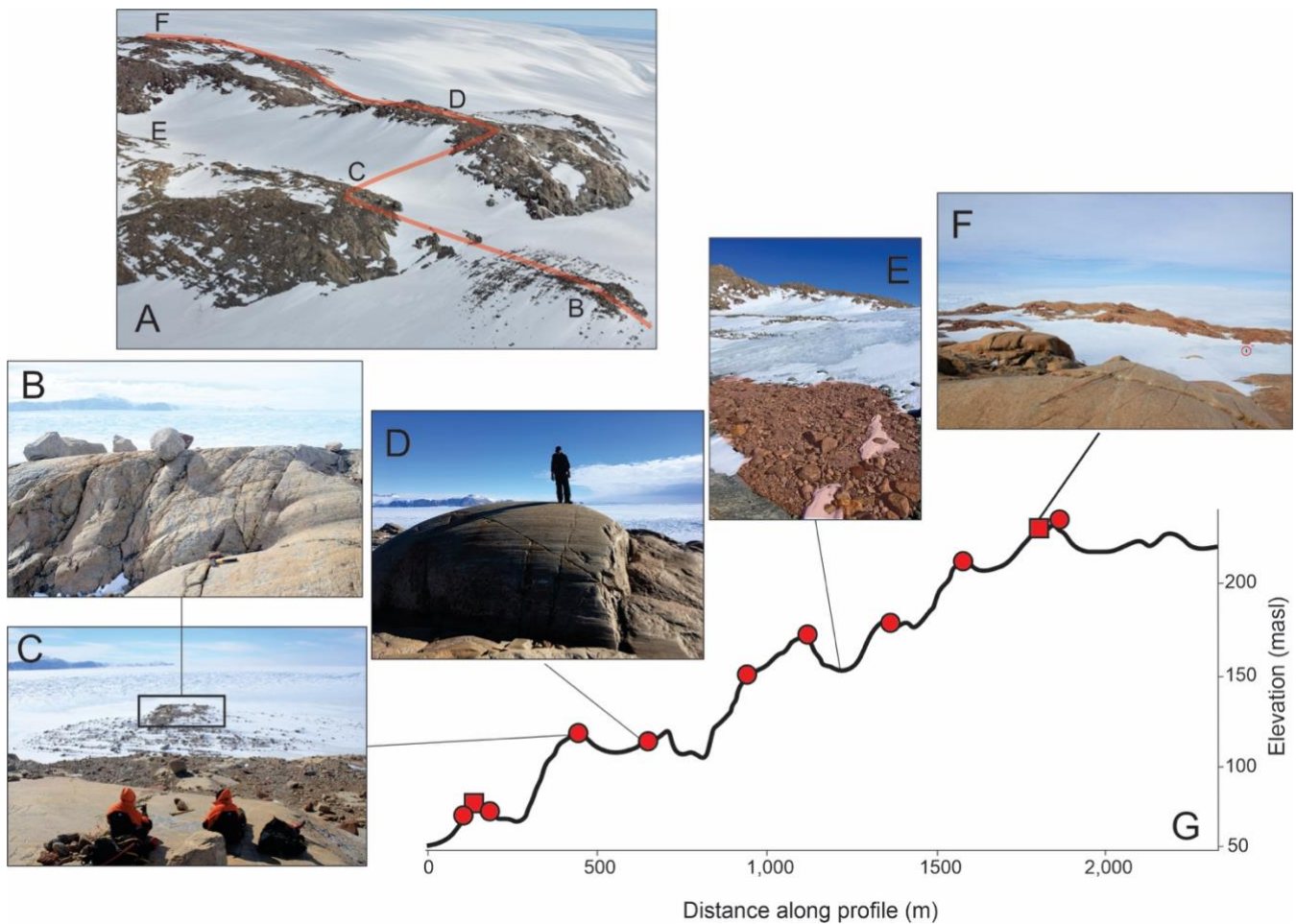
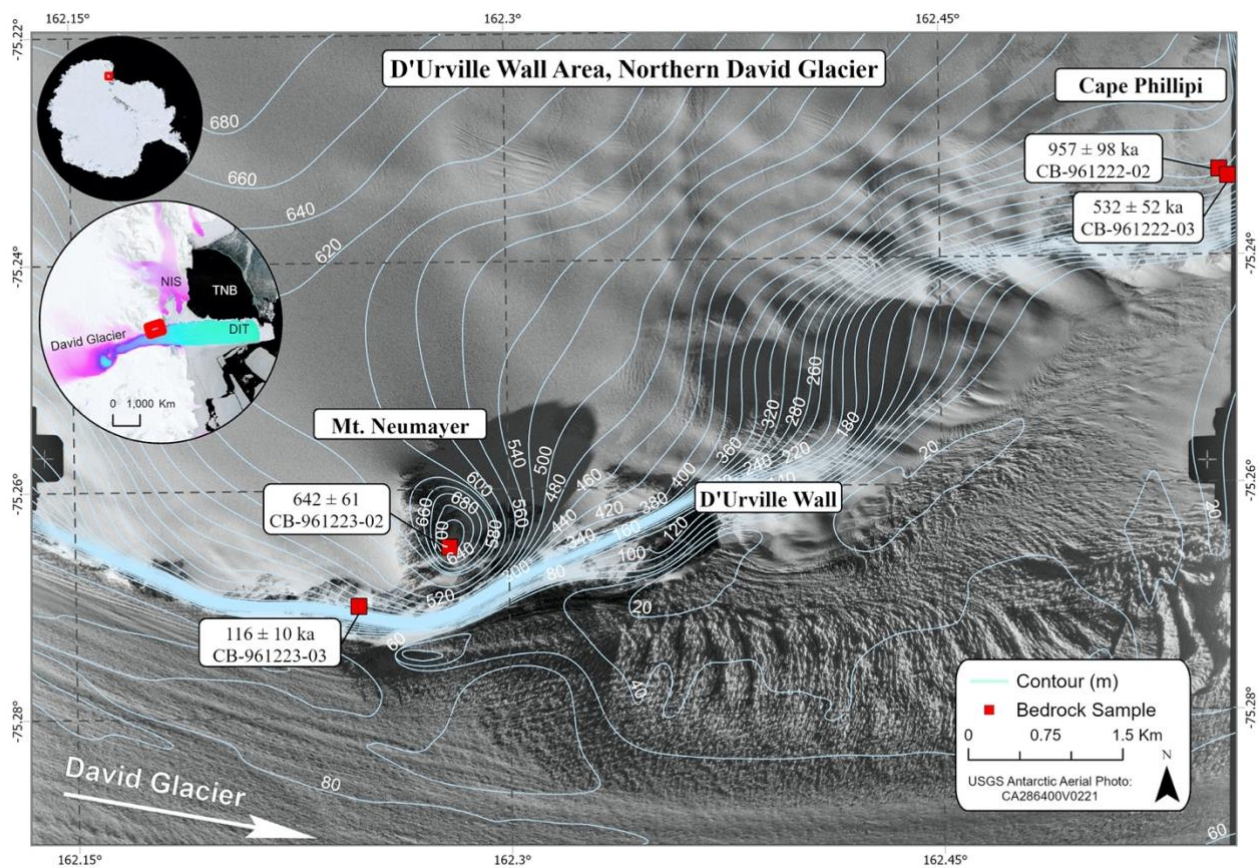
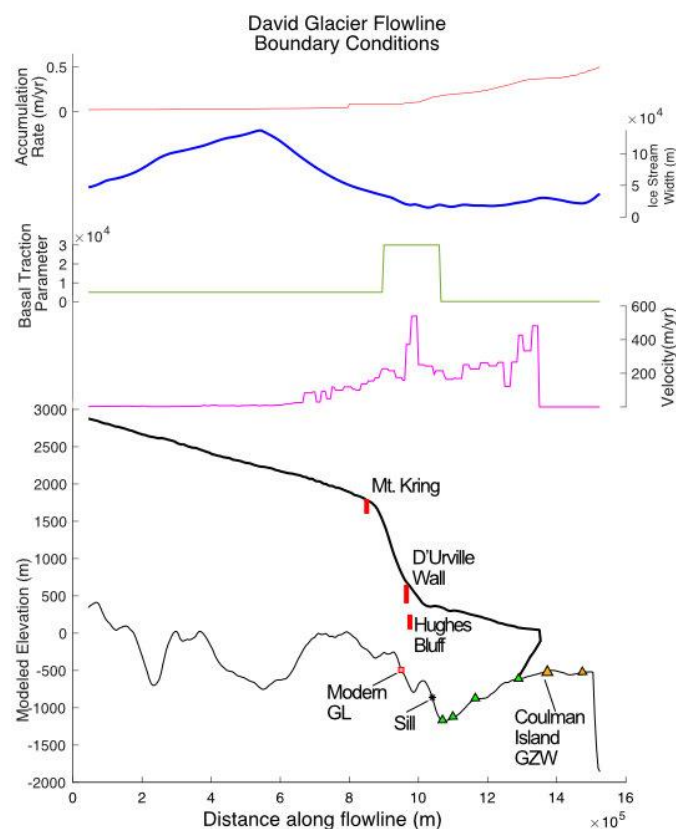


Figure S4: A) West facing oblique aerial photo of Hughes Bluff with approximate location of topographic profile (red), (B) North facing view from low bedrock knob showing perched glacial erratics and location of lowest emergent bedrock knob, (C) North facing view of moulded, striated and grooved nature of bedrock at lowest outcrop of Hughes Bluff, (D) North facing view of spectacular roch  s moutonn    s observed throughout Hughes Bluff, (E) West facing view of 'cold till' observed in multiple localities along small scale channel forms (outlined in red), (F) Highest elevation outcrop of Hughes Bluff showing rounded summit morphology with glacial striations, view to east. (G) Topographic profile from SfMP showing representative sampling sites (red circles for erratics and red squares for bedrock samples).





40 Figure S5: Map of D'Urville Wall area with all bedrock exposure ages ( $^{10}\text{Be}$ ) with total errors listed. Aerial photo courtesy USES Antarctic Single Frames accessed through USGS Earth Explorer (<https://earthexplorer.usgs.gov/>). Elevation contours of Howat et al., 2018. Large inset shows surface velocity of Rignot et al., (2011) and small inset shows LIMA data of Bindshadler et al., (2008). DIT=Drygalski Ice Tongue, TNB=Terra Nova Bay and NIS=Nansen Ice Shelf.



45 Figure S6: Boundary conditions along flowline distance used for deglacial modelling experiments in this study. Inputs include basal topography of Fretwell et al., (2013) and Arndt et al., (2013), modelled palaeo-ice surface and velocity of Whitehouse et al. 2012 and accumulation of VanWessem et al., (2018). Mapped grounding zone features (orange triangles with age constraints, green triangles of Lee (2019) without age constraints), topographic features, modern day grounding line and terrestrial sites discussed in text are plotted along the upper ice surface and basal topography